The 2009 IEEE/RSJ International Conference on
Intelligent Robots and Systems
October 11-15, 2009 St. Louis, USA

Achieving Three-Dimensional Automated Micromanipulation at the Scale of Several Micrometers with a Nanotip Gripper

Hui Xie, *Member, IEEE,* Juan Camilo Acosta, *Student Member, IEEE,* and Stéphane Régnier

***Abstract*—Three-dimensional (3-D) automated micromanipulation at scale of several micrometers using a nanotip gripper is presented. The gripper is constructed from protrudent tips of two independently actuated atomic force microscope (AFM) cantilevers and each cantilever. A protocol allows these two cantilevers to form a gripper for grasping and releasing the microspheres to target positions without obstacle of adhesive forces in air. For grasping, amplitude feedback from the dithering cantilevers is employed to locate the grasping points by laterally scanning the side of the microspheres. Real time force sensing is used to monitor the whole process of the pick-and-place with steps of pickup, transport and release. For trajectory planning, an algorithm based on the shortest path solution is used to obtained 3-D micropatterns with high efficiencies. In experiments, microspheres with diameters from 3 μm to 4 μm were manipulated and 3-D micropyramids with two layers were achieved. 3-D micromanipulation and 3-D microassembly at the scale of several microns to submicron could become feasible through the newly developed nanotip gripper.**

I. Introduction

MICROMANIPULATION, as one of significant techniques in fabrication of three-dimensional (3-D) microstructures and in applications of biology, has been investigated over one decade. Up to now, many research efforts have been made to build microstructures [1–3], fabricate photonic devices [4] and scientific explorations in biology [5–8]. In order to build two-dimensional (2-D) or 3-D microstructures and complete manipulation of biology samples, various end-effectors have been proposed: pushing and pulling with a nanoprobe [9], pick-and-place using microgrippers [10–15], a microcantilever [16], collaborating fingers [17] and noncontact tools such as the optical gripper [18].

It is well known that the pick-and-place is a significant manipulation technique on 3-D microstructure fabrication since it is an indispensable step in the bottom-up building process. However, few literatures reported the mechanical pick-and-place manipulation of microobjects with feature sizes less than 10 μm, especially the manipulation confined in air. The main difficulties in sufficiently completing the pick-and-place micromanipulation at this scale are in fabricating such a sharp end-effectors that has a capability of smoothly releasing microobjects, simultaneously with an enough output of grasping force to overcome strong adhesion forces [19–21] as well as capabilities of sensing and control of interactions between the microobject and the tool or the substrate. Furthermore, compared with the larger microobjects, optical vision feedback on several microns suffers more from shorter depth-of-focus and narrower field-of-view using lenses with higher magnifications, although different schemes or algorithms have been introduced on the optical microscope for autofocusing [22], [23] and extension of the depth-of-focus [24]. In contrast with the vision-servoing based 2-D automated micromanipulation [9], automated 3-D micromanipulation at the scale of several microns is still a great challenge in building 3-D microstructures due to the lack of sufficient feedback information that is beyond the capability of the microscopic vision, such as the vertical contact detection along the optical axis or manipulation obstructed by opaque components. Thus, in order to facilitate the 3-D micromanipulation at the scale less than 10 μm, multi-feedback is of vital importance to achieve such an accurate and stable 3-D micromanipulation.

In this paper, in order to achieve the 3-D manipulation of microobjects with feature sizes from submicron to 10 μm, an atomic force microscope (AFM) based 3-D micromanipulation system (3DMS) with a nanotip gripper is developed. This system can be used to build 2-D micropatterns by pushing and pulling microobjects on a single plane, and, more importantly, to achieve the pick-and-place micromanipulation with sufficient interaction force sensing. The 3DMS mainly consists of two collaborating AFM cantilevers with protrudent tips and two corresponding nanopositioning and optical levers. A nanotip gripper is constructed by these two tips to achieve a procedure of 3-D micromanipulation with general steps of contact detecting, grasping, picking up, transporting and releasing. We have used the developed 3DMS to fabricate five micropyramids with two layers by manipulating microspheres with diameters of 3 μm $\sim$ 4 μm. Compared with other means of pick-and-place micromanipulation in air, the developed 3DMS is more controllable due to the real time interactive force sensing, and without obstacle on the microsphere releasing due to very sharp tips of the gripper.

II. System Configuration of the 3DMS

As shown in Fig. 1(a) and (b), the proposed 3DMS is equipped with an optical microscope and two sets of similar devices commonly used in a conventional AFM, including two cantilevers (ATEC-FM) with corresponding nanopositioning devices and optical levers. The optical levers, typically composed of a laser and a quadrant photodiode that is believed to be more sensitive and reliable detection device than other means [25], are arranged on two vertical planes and used to detect actions of both cantilevers, as seen in Fig. 1 (b). The bottom inset of Fig. 1 (c) shows that the protrudent tip of each cantilever has an tilted angle about 70° on the side view. These tips are employed as end-effectors to build a nanotip gripper

Manuscript received March 1, 2009; This work has been supported by the French National Agency of Research, through the PACMAN and NANOROL projects.

Authors are with the Institut des Systèmes Intelligents et Robotique (ISIR), Université Pierre et Marie Curie–Paris VI/CNRS, 4 Place Jussieu, 75005 Paris, France. (e–mail: xie@robot.jussieu.fr) .

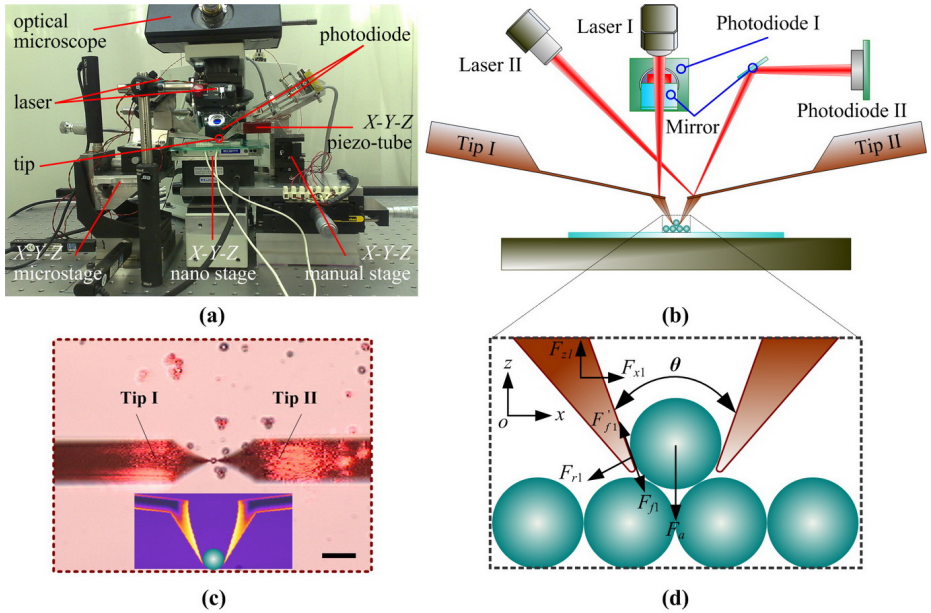

Fig. 1. (a) A photo of the 3DMS. (b) System configuration of the 3DMS. (c) A microscopic image captured during the pickup operation of a microsphere using the nanotip gripper. The bottom insert shows the pick-and-place manipulation scheme with a nanotip gripper. The scale bar represents 20 μm. (d) A zoomed figure shows the scheme of grasping operation with a nanotip gripper.

with a clamping angle of $40°$, as shown in Fig. 1(d). The nanotip gripper is used to pick up and place the microobject to its target position. The configuration of the 3DMS can be described as follows:

1) Cantilever I, which is immovable during the micromanipulation, is fixed on an *X–Y–Z* micropositioning stage for coarse positioning. The normal stiffness of Cantilever I and the sensitivity of its optical lever are calibrated as 2.43 N/m and 0.65 nm/mV, respectively.
2) Cantilever II is actuated for grasping operations by an *X–Y–Z* piezotube (PI P–153.10H) with a scan range of 10 μm and a resolution of sub–nanometer on each axis. The piezotube is well compensated by the Prandtl–Ishlinskii operator on its hysteresis[26] and mounted on an *X–Y–Z* manual microstage. The normal stiffness of Cantilever II and the sensitivity of its optical lever are calibrated as 2.48 N/m and 0.58 nm/mV, respectively.
3) An *X–Y–Z* nanostage (MCL Nano–Bio2M on the *X–Y* axes, PI P–732. ZC on the *Z*–axis) with a maximum motion range of 50 μm $\times$ 50 μm $\times$ 10 μm and a closed-loop resolution of 0.1 nm is employed to support and transport samples.
4) A data acquisition card (NI 6289) with a resolution of 18 bits in A/D transfer and a maximum sampling frequency of 625 kHz is used for data acquisition from the optical levers and actuate the *X–Y–Z* piezotube by exporting voltage signals to three independent amplifiers.

III. Pick-and-Place Micromanipualtion Schemes

A. Manipulation Protocol of the 3DMFM

Microparticles and microspheres are being intensively investigated as significant experimental materials for micromanipulation. Thus, a protocol of the 3DMS is made for a specific application of the microparticles or microsphere deposited on the substrate. However, applications of such a protocol can also be extended to the pick-and-place operation of other types of microobjects dispersed on the substrate. As shown in Fig. 2, a procedure of the pick-and-place mainly involves:

1) System Initialization: Set each axis of the nanostage and the piezotube on a proper position, providing the pick-and-place operation with enough displacement on each axis.

2) Trajectory Planning: Trajectory planning is started after an image processing of a global view that contains all the microspheres to be manipulated. In our method, image is just utilized to detect coarse positions of microspheres, providing a distribution of all the microspheres for the trajectory planning and subsequently, fine positioning of each microsphere will be fulfilled with amplitude or force feedback from the cantilevers, which will be discussed in the next section.

3) Contact with Tip I: As seen in Fig. 2 (a), keeping a gap between the dithering Tip I and the substrate when it is approaching to the microsphere by moving the piezotube on the *X*–axis. An actual grasping point and contact on the microsphere can be detected by the amplitude feedback, which will be discussed in Section *D* of Part III.

4) Contact with Tip II: As Tip I is in contact with the microsphere, contact between Tip II and the microsphere is also achieved in Fig. 2 (b) by following the process in the last step, building a nanotip gripper in Fig. 2 (c).

5) Pick up, Transport and Place: Once the grasping is ready, as shown in Fig. 2 (d), the microsphere is picked up, transported and placed by moving nanostage on each axis with proper displacements that depend on the location of the destination and the size of the microsphere. The whole procedure of the 3-D micromanipulation is monitored by the real time force sensing.

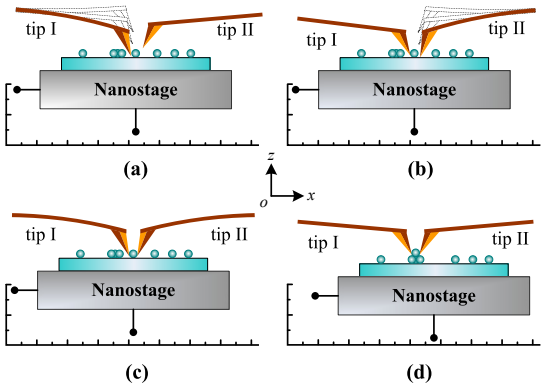

Fig. 2. Protocol of the pick-and-place operation of microspheres. Four main steps are involved. The dithering Tip I is used to locate the grasping point by local scanning with amplitude feedback (a). In the step (b), the grasping point between Tip II and the microsphere is detected with the dithering Tip II. The grasping operation is ready for pickup as both tips contact with the microsphere. The pick-up manipulation is achieved in step (c) by moving the nanostage on the *Z*–axis. (d) A micropyramid is fabricated as the microsphere is placed on the first microsphere layer.

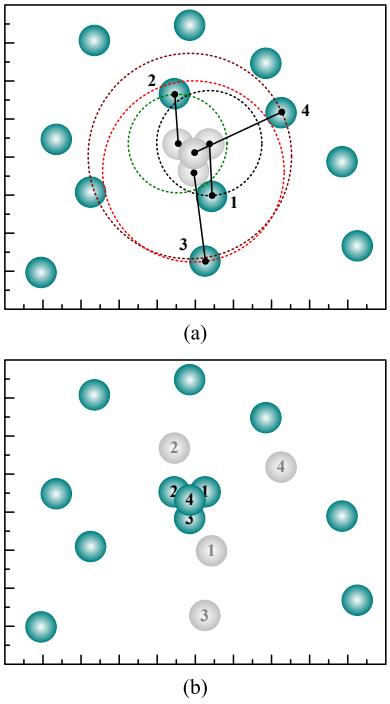

Fig. 3. Simulated 3-D assembly of a micropyramid constructed with four microspheres using shortest path algorithm, in which numbers depict the order of the manipulation. (a) Before manipulation. (b) After manipulation.

B. Trajectory Planning for Pattern Formation

Unlike a trajectory planning on 2-D pushing/puling micro-manipulation [9], the blockage problem in trajectory planning is eliminated in our system since the microspheres are picked up with heights above all the microobjects on the substrate before the transport. In this case, an algorithm, based on the shortest path solution, is developed for a linear trajectory planning on a pattern formation. As a manipulation example shown in Fig. 3, the planning is described as follows:

1) Capture a frame of gray microscopic images.
2) Detect central position of each microsphere in the image space utilizing method adopted in [9].
3) Determine target positions and manipulation sequences.
4) **for** $n = 1$ to N (number of targets).
   a) Generate all possible linear trajectories between each microsphere and the target position $t_n(x, y)$.
   b) Select the microsphere with a central position $o_n(x, y)$ that has the shortest path to the target position, as show in Fig. 3 (a).

   end for
5) Transform the position sequences $t_n(x, y)/o_n(x, y)$ from the image space into $T_n(x, y)/O_n(x, y)$ within the nanostage motion space for a actual motion planning.

C. Grasping Point Searching and Contact Detection

As shown in Fig. 4 (a), the dithering cantilever with the first mode of oscillation is utilized to search grasping points on the diameter of the contact circle of the microsphere and detect the contact using real time amplitude feedback. As shown in the insert I of Fig. 4 (a), the dithering cantilever sweeps on the *Y*–axis with distance about half of the microsphere diameter when it is approaching the microsphere with a gap of 500 nm to the substrate. When the tip laterally taps on the microsphere, the grasping point can be accurately located by searching for the minimum amplitude response. A corresponding experimental result can be found in the Fig. 4 (b), in which the tip laterally sweeps the microsphere within a range of 1.6 μm with a free oscillating amplitude of 320 nm. Six different distances to the microsphere from 120 nm to 20 nm were tested and ultimately, the grasping point is well located with an accuracy of $\pm$10 nm that is in much excess of the resolution the optical microscope. As the scheme depicted in insert II of Fig. 4 (a), amplitude feedback is also used for contact detection. As seen in Fig. 4 (c), contact between the tip and the microsphere is achieved as the amplitude reduces to a steady value near zero. When the dithering tip returns to its natural amplitude, a hysteresis loop is induced from the transitions between adhesive and repulsive forces between the tip and the microsphere [27]. In addition, contact can be also detected by the normal force response from the cantilever. As shown in Fig. 4 (d), a full normal force response in an approach-retraction loop can be recognized by steps of snap-in, contact and pull-off, which is usually in the presence of the tip-substrate contact. In our experiments, as the contact between Tip I and the microsphere is ready, Tip I retraces 5–10 nm in order to keep a tiny gap between Tip I and the microsphere. This gap enables a smart recognition of grasping state as Tip II contact with the microsphere with a slightly further push. Compare with operations under the optical microscope, the amplitude detecting method has two obvious advantages: 1) Grasping point and contact can be detected below the opaque components, more importantly, with accuracy that is far beyond the capability of the microscope. 2) Benefiting from the accurate force and amplitude measuring of the optical lever, the grasping points and contact can be accurately detected with very weak interactions at the scale of nano-Newton, protecting the fragile tips and microobjects from damage.

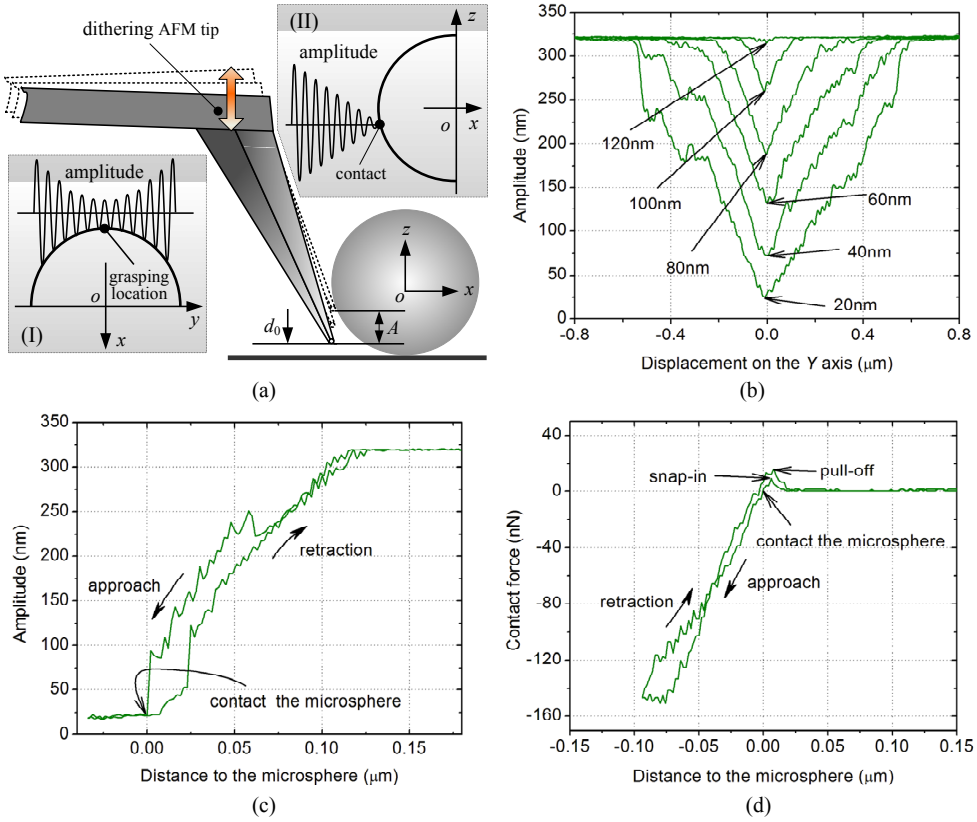

Fig. 4. Schemes and experimental results of grasping point searching and contact detection on a microsphere. (a) Schematic of grasping points locating (insert I) and contact detection (insert II) using the amplitude feedback. A is the amplitude and d_0 is the distance between the tip and the substrate. (b) Amplitude responses of the cantilever when it is sweeping on the Y–axis with different distance from the microsphere on the X–axis. (c)Amplitude responses of the cantilever when it is approaching the contact point on the microsphere. (d)Normal force responses could also be employed for the contact detection.

D. Force Sensing During pick-and-place

In order to measure the interactive forces between the tips and the microsphere during the procedure of the pick-and-place, as shown in Fig. 1 (d), the interactive forces on Tip I can be measured as a normal signal from the well-calibrated photodiode by the following equations:

$$\begin{cases} F_{z1} = F_{f1}\cos\theta/2 + F_{r1}\sin\theta/2 \\ F_{x1} = F_{r1}\cos\theta/2 - F_{f1}\sin\theta/2 \end{cases} \tag{1}$$

where F_{z1} and F_{x1} are the bending forces applied respectively on the Z–axis and the X–axis, F_{r1} is a repulsive force and F_{f1} is a friction force between Tip I and the microobjects. In the actual use, a clamping angle 40° and a normal $\mu = 0.3$ are used [28]. Thus, from (1), F_{z1} and F_{x1} can be solved as $F_{z1} = 0.623F_{r1}$ and $F_{x1} = 0.837F_{r1}$. The bending angular deformation ϕ associated with a torque M applied on the end of the cantilever can be calculated as:

$$\phi = \frac{ML}{2EI} \tag{2}$$

where L is the beam length of the AFM cantilever, E is Young's modulus of the cantilever, I is moment of inertia on the cantilever's cross-section area. A torque M_1 generated from the F_{z1} with a long turning lever of the cantilever length $L = 225$ μm. In contrast, the torque M_2 generated from the F_{p1} is just with turning lever of the tip length 10 μm. From (2), the cantilever moments associated with the normal signal output of the photodiode can be estimated as $M_2 \leq 0.06M_1$. Thus, the contribution of from the F_{x1} can be neglected. Therefore, the F_{p1} can be simplified estimated as $F_{z1} = \beta_1 \cdot \Delta V_1$, where β_1 is the normal force sensitivity of the optical lever on Tip I, ΔV_1 is the voltage response of the photodiode due to the force load. A similar result can be deduced on Tip II. Once the F_{z1} and F_{z2} are known, the adhesion force on the nanoobject F_a can be estimated as:

$$F_a = F_{z1} + F_{z2} = \beta_1\Delta V_1 + \beta_2\Delta V_2 \tag{3}$$

where β_2 and ΔV_2 are the normal sensitivity and the voltage output on Tip II, respectively.

Fig. 5 shows a full force spectroscopy curve during the pick-and-place operation of a microsphere deposited on the glass slide with an environmental temperature of $20°C$ and relative humidity of 38%. The force spectroscopy curve is synthesized from force responses on both tips. The curve starts from contact state between the microsphere and the substrate. During the pickup, when the nanostage position reaches -170 nm, the gripper-microsphere pulls off the substrate with a pull-off force of 746 nN. After this, the force curve returns to -220 nN other than the initial force due to the contribution of friction forces between the gripper and the microsphere. The insert I shows that the microsphere relatively slides down from the gripper during the pick-up operation, which leads to

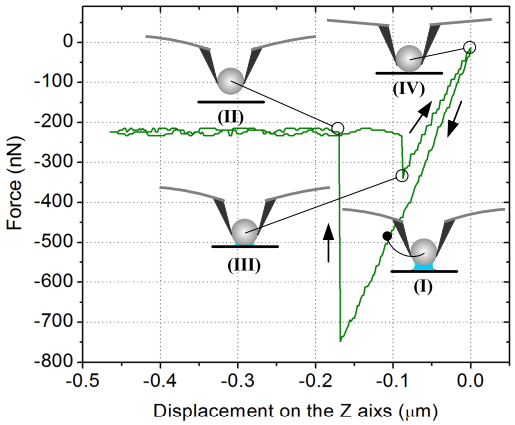

Fig. 5. Synthesized normal force responses on both microcantilevers during the pick-and-place manipulation of a microsphere. (I) pick-up. (II) Pull-off. (III) Snap-in. (IV) Contact on the retraction branch.

a bending deformations kept by the frictions on the nanotips (insert II). During the retracting branch, an earlier snap-in occurs with a distance of about 50 nm to the starting point, indicating that the microsphere slides with the same distance during the pick-up operation (insert III). Further retraction leads to a continue increase with a higher slope than that of the pick-up until both the nanostage position and the magnitude of the normal force get back to the initial grasping state (insert IV). Once such a force spectroscopy curve occurs during the pick-and-place manipulation, a stable grasping as well as a successful releasing operation could be validated.

IV. Experimental Results and Discussion

A. Task Description

In order to validate the manipulation ability of the developed 3DMS, nylon microspheres with diameter of 3 μm $\sim$ 4 μm were manipulated in our experiments. The nylon microspheres were deposited on a newly cleaned glass slide and then an interesting area for experiments was selected under the optical microscope with a 20$\times$ objective. Fig. 6 shows a top image view of the selected area, in which more than 24 microspheres are included and 20 of them separated by a frame of 56 μm square. They are going to be manipulated to build five microsphere pyramids labeled by assembly sequences from I to V. Each pyramid is constructed by four microspheres with two layers. The bottom inserts show two types of assembly sequences depicted by numbers for two different arrangements of the pyramids. Tip I and Tip II, with a laser spot focused on each cantilever's end, are located beside the manipulation area after system initialization, which is in convenience of trajectory planning. After trajectory planning, 3D microassembly task is carried out with the predefined sequences to build five micropyramids, as schematic structures constructed by the green spheres.

B. Manipulation Results

Fig. 7 shows the 3-D micromanipulation process of the micropyramids. Fig. 7 (a) and (b) are captured when the first

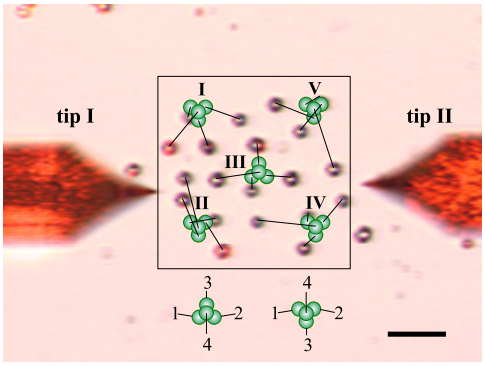

Fig. 6. Optical microscope image before the pick-and-place micromanipulation. Twenty microspheres with diameter of 3 μm $\sim$ 4 μm will be manipulated in building five microsphere pyramids (labeled from I to V). The bottom inserts show two types of assembly sequences depicted by numbers. The scale bar represents 15 μm.

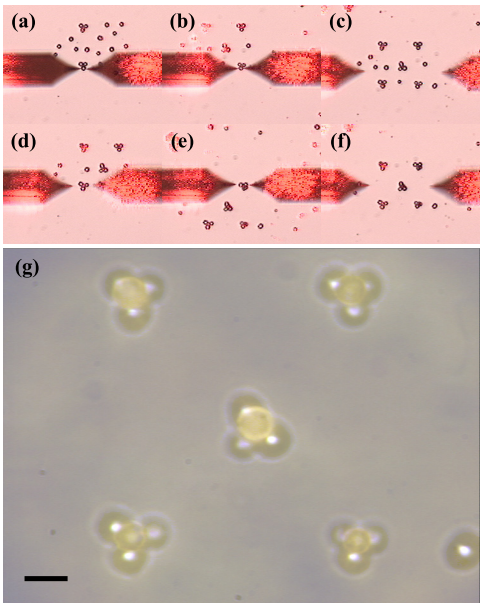

Fig. 7. Assembly results. (a)–(c) show three images intercepted from assembly process of the first layer of the micropyramids. (d)–(f) depict assembly process of the second layer of the micropyramids. The images (a)–(f) are captured under magnification of 20$\times$. (g) The 3D microassembly results under magnification of 100$\times$, in which the scale bar represents 5 μm.

layer of the pyramid II and VI are assembled, respectively. The image in Fig. 7 (c) is captured as the first layer of the five pyramids has been completed, in which twenty microspheres have been placed on the reference positions with pick-and-place operation. Once the first layer is ready, the remaining five microspheres are sequentially picked up and placed on each reference positions on the second layer. Fig. 7 (d) and (e) describe the transporting process of the twenty-first and the last microsphere, respectively. The ultimate result is shown in Fig. 7 (f). In addition, the assembly result is displayed more distinctly under the microscope with a 100$\times$ objective, as seen in Fig. 7 (g). Concerning about more details, several aspects of the microassembly should be explained as follows.

As the AFM tip radius is about 10 nm, with respect to the microsphere-substrate contact, the microsphere-tip contact

area is much smaller, which leads to tiny adhesion forces between the gripper and microsphere. However, in order to achieve smoothly releasing operation, firstly, it is should make certain the tip–microsphere contact with only the tips of the AFM cantilevers by reserving a proper distance between the gripper tip and the substrate in grasping. Moreover, it is of significant importance to ensure a full microsphere–substrate contact by waiting for several seconds before opening the nanotip gripper for the releasing. In addition, the tips should keep dithering in its natural resonance during the whole procedure of pick-and-place manipulation, especially in the process of releasing, for a purpose of reducing adhesion forces between the gripper and the microsphere due to great inertial forces applied to the microsphere [17]. By applying schemes or strategies mentioned above, obstacle of sticking is estimated in our pick-and-place experiments with microspheres less than 4 μm in diameter.

In addition, note that several interrupts occurred with user's intervenes for the nanotip gripper relocation during the whole microassembly of the five micropyramids due to the constraint of the limited motion range 50 μm $\times$ 50 μm of the nanostage, which is less than the manipulation range of 56 μm $\times$ 56 μm. The gripper relocating is completed by moving the microstage and the manual stage that are used to support Tip I and Tip II, respectively. However, each single pick-and-place operation is definitely fulfilled with an automated way.

V. Conclusion

It is well known that the pick-and-place micromanipualtion is with a great challenge for microobjects with feature sizes less than 10 μm, especially for the manipulation confined in air. Fortunately, the newly developed 3DMS has achieved this type of pick-and-place micromanipulation with a nanotip gripper constructed by two AFM cantilevers. In order to validate the manipulation ability of the 3DMS, microspheres with diameter less than 4 μm were manipulated and as a result, five micropyramids have been built. The 3DMS has made the automated 3-D micromanipulation and microassembly at several micrometers in air feasible. In our future work, efforts will be made to scale down the manipulation object to sub-micrometers and ultimately, to applications at nanoscale, which need us to solve several issues, such as strategies or schemes in overcoming severe sticking problems in this scale and compensation of positioning errors due to thermal drift.

References

[1] N. Dechev, M. L. Cleghorn, and J. K. Mills, "Microassembly of 3-D Microstructures Using a Compliant, Passive Microgripper," *J. Microelectromech. Syst.*, vol. 13, no. 2, pp. 176–189, 2004.

[2] H. Xie, W. B. Rong, and L. N. Sun, "A flexible experimental system for complex microassembly under microscale force and vision-based control," *Int. J. Optomechatro.*, vol.1, no. 1, pp. 81–102, 2007.

[3] G. Yang, J. A. Gaines, and B. J. Nelson, "A Supervisory Wafer-Level 3D Microassembly System for Hybrid MEMS Fabrication," *J. Intell. Robot. Syst.*, vol. 37, no. 1, pp. 43–68, 2003.

[4] K. Aokil, H. T. Miyazakl, H. Hirayama, K. Inoshita, T. Baba, K. Sakoda, N. Shinya, and Y. Aoyagl, "Microassembly of semiconductor three dimensional photonic crystals," *Nat. mater.*, vol. 2, no. 2, pp. 117–121, 2003.

[5] W. H. Wang, X. Y. Liu, D. Gelinas, C. B. Brian, and Y. Sun, "A Fully Automated Robotic System for Microinjection of Zebrafish Embryos," *Plos ONE*, vol. 2, no. 9, pp. e862, 2007.

[6] Z. Lu, P. C. Y. Chen, J. Nam, R. W. Ge, and W. Lin, "A micromanipulation system with dynamic force-feedback for automatic batch microinjection," *J. Micromech. Microeng.*, vol. 17, no. 2, pp. 314–321, 2007.

[7] M. Gauthier, and E. Piat, "Control of a particular micro–macro positioning system applied to cell micromanipulation," *IEEE T. Autom. Sci. Eng.*, vol. 3, no. 3, pp. 264–271, 2006.

[8] Y. Marcy, J. Prost, M. F. Carlier, and C. Sykes, "Forces generated during actin–based propulsion: A direct measurement by micromanipulation," *P. Natl. Acda. Sci. USA*, vol. 101, no. 16, pp. 5992–5997, 2004.

[9] C. D. Onal, and M. Sitti, "Visual servoing–based autonomous 2–D manipulation of microparticles using a nanoprobe," *IEEE T. Contr. Syst. Tech.*, vol. 15, no. 5, pp. 842–852, 2007.

[10] N. T. Nguyen, S. S. Ho, and C. L. N. Low, "A polymeric microgripper with integrated thermal actuators," *J. Micromech. Microeng.*, vol. 14, no. 7, pp. 969–974, 2004.

[11] O. Millet, P. Bernardoni, S. Régnier S, P. Bidaud, E. Tsitsiris, D. Collard, and B. L. Lionel, "Electrostatic actuated micro gripper using an amplification mechanism," *Sensor Actuat A: Phys.*, vol. 114, no. 2–3, pp. 371–378, 2004

[12] C. Clévy, A. Hubert, J. Agnus, and N. Chaillet, "A micromanipulation cell including a tool changer," *J. Micromech. Microeng.*, vol. 15, no. 10, pp. S292–S301, 2005.

[13] M. C. Carrozza, A. Eisinberg, A. Menciassi, D. Campolo, S. Micera, and p. Dario, "Towards a force–controlled microgripper for assembling biomedical microdevices," *J. Micromech. Microeng.*, vol. 10, no. 2, pp. 271–276, 2000.

[14] A. Neild, S. Oberti, F. Beyeler, J. Dual, and B. J. Nelson, "A micro–particle positioning technique combining an ultrasonic manipulator and a microgripper," *J. Micromech. Microeng.*, vol. 16, no. 8, pp. 1562–1571, 2006.

[15] X. Y. Kim, X. Y. Liu, Y. Zhang, and Y. Sun, "NanoNewton force–controlled manipulation of biological cells using a monolithic MEMS microgripper with two–axis force feedback," *J. Micromech. Microeng.*, vol. 18, no. 5, pp. 055013, 2008.

[16] D. S. Haliyo, F. Dionnet, and S. Régnier, "Controlled rolling of microobjects for autonomous manipulation," *J. Micromechatro.*, vol. 3, no. 2, 75–101, 2006.

[17] W. Driesen, T. Varidel, S. Régnier, and J–M Breguet, "Micro manipulation by adhesion with two collaborating mobile micro robots," *J. Micromech. Microeng.*, vol. 15, no. 10, pp. S259–S267, 2005.

[18] I. Y. Park, S. Y. Sung, J. H. Lee, and Y. G., "Manufacturing micro–scale structures by an optical grippers system controlled by five finger tips," *J. Micromech. Microeng.*, vol. 17, no. 10, pp. N82–N89, 2007.

[19] A. Menciassi, A. Eisinberg, I. Izzo, and P. Dario, "From 'Macro' to 'Micro' Manipulation," *IEEE–ASME T. Mechatro.*, vol. 9, no. 2, pp. 311–320, 2004.

[20] P. Lambert, and S. Régnier, "Surface and contact forces models within the framework of microassembly," *J. Micromechatro.*, vol. 3, no. 2, pp. 123–157, 2006.

[21] M. Sitti, "Microscale and nanoscale robotics systems–Characteristics, state of the art, and grand challenges," *IEEE Robot. Autom. Mag.*, vol. 14, no. 1, 53–60, 2007.

[22] H. Xie, W. B. Rong, and L. N. Sun, "Construction and Evaluation of a Wavelet–Based Focus Measure for Microscopy Imaging," *Microsc. Res. Techniq.*, vol. 70, no. 11, pp. 987–995, 2007

[23] X. Y. Liu, W. H. Wang, and Y. Sun, "Dynamic evaluation of autofocusing for automated microscopic analysis of blood smear and pap smear," *J. Microsc.*, vol. 227, no. Pt1, pp. 15–223, 2007.

[24] H. Xie, W. B. Rong, L. N. Sun, and W. Chen, "Image fusion and 3-D surface reconstruction of microparts using complex valued wavelet transforms," *IEEE Intl. Conf. Image. process*, Atlanta GA, pp. 2137–2140, 2006.

[25] G. Meyer, and N. M. Amer, "Novel optical approach to atomic force microscopy," *Appl. Phys. Lett.*, vol. 53, no. 12, pp. 1045–1047, 1998.

[26] P. Krejci, and K. Kuhnen, "Inverse control of systems with hysteresis and creep," *IEE Proc–Control Theory Appl.*, vol. 148, no. 3, 185–192, 2001.

[27] R. Garcia, and R. Perez, "Dynamic atomic force microscopy methods," *Sur. Sci. Rep.*, vol. 47, no. 6–8, pp. 197–301, 2002.

[28] M. Varenberg, I. Etsion, and G. Halperin, "An improved wedge calibration method for lateral force in atomic force microscopy" *Rev. Sci. Instrum.*, vol. 74, no. 7, pp. 3362–3367, 2003.